Published in final edited form as:
Biochem Biophys Res Commun. 2008 June 13; 370(4): 613–618. doi:10.1016/j.bbrc.2008.03.147.

Rational design of minimal hypoxia-inducible enhancers

Stefan Kaluz*, **Milota Kaluzová**, and **Eric J. Stanbridge**
Department of Microbiology and Molecular Genetics, Medical Science I, B210, University of California at Irvine, College of Medicine, CA 92697-4025, USA

Abstract

The hypoxia-inducible factor (HIF) activates transcription via binding to the highly variable hypoxia-responsive elements (HREs). All hypoxia-inducible constructs described to date utilize multimers of naturally occurring HREs. Here, we describe the rational design of minimal hypoxia-inducible enhancers, conceptually equivalent to using an optimized HIF-binding site (HBS) as the building block. Optimizations of the HBS, spacing between HBSs, the distance from the minimal promoter, and orientation of HBSs allowed us to design constructs with high hypoxic activity. Activation of the 4xopt HBS (36 bp) construct by hypoxia or HIF-1α and HIF-2α was comparable with that of the 4x*EPO* HRE (208 bp) construct. The strong synergism between the properly arranged optimized HBSs was due to stimulation of high affinity HIF binding. Our data prove, for the first time, that it is possible to assemble artificial hypoxia-inducible enhancers from a single type of regulatory element-optimized HBS.

Keywords

Hypoxia; Hypoxia-inducible factor; Hypoxia responsive element; HIF-binding site

The hypoxia-responsive element (HRE) is a minimal *cis*-regulatory element mediating transactivation by the hypoxia-inducible factor (HIF) [1]. The data from over 70 genes suggest that endogenous HREs are composite regulatory elements comprising the conserved HIF-binding site (HBS) with an A/GCGTG core sequence and a highly variable flanking sequence. A single HBS is necessary but not sufficient for activation by hypoxia and the flanking sequence provides binding sites for transcription factors that are not necessarily hypoxia-inducible but are required to amplify the hypoxic response or make the HRE tissue-specific [1]. In contrast to our knowledge of regulation of the HIF pathway, relatively little progress has been made towards understanding the fundamental structural features of HREs. There are only a few reports relating the sequence of HRE with activity, e.g. mutational analysis of the −2 position of HBS revealed that hypoxic induction decreases in the T ≫ G > C order [2,3].

Direct consequence of our limited understanding of HRE is that all hypoxia-inducible constructs for therapeutic or monitoring purposes described to date are based on multimers of naturally occurring HREs, ranging from 24 bp for murine *phosphoglycerate kinase-1* (m*PGK1*) [4], 35 [5] or 44 [6] bp for *erythropoietin* (*EPO*), and 37 bp for *vascular endothelial growth factor* (*VEGF*) [5] HREs. Apparently, the progress towards optimized HREs has been hampered by two major factors: the fact that HREs come in different “flavors”, significantly diverging from each other [1] and the complexity of regulation by hypoxia, highlighted in the m*LDHA* promoter where mutations at three separate sites abolished hypoxic induction [7]. Moreover, concatamerization of any of the three functionally critical sites did not confer high-

*Corresponding author. Fax: +1 949 824 8598. E-mail address: skaluz@uci.edu (S. Kaluz).

level hypoxic induction, leading to the conclusion that each site is necessary but not sufficient on its own for hypoxic induction [7].

Our goal in this study was to rationally design minimal hypoxia-inducible enhancers, defined as the minimal number of the shortest possible building blocks. The basic structural organizations of HRE were inferred from the sequences of naturally occurring HREs with the highest hypoxic induction. This information, combined with optimizations at several levels, allowed us to assemble short, highly inducible artificial enhancers exclusively from HBSs.

Materials and methods

Plasmid constructions

Wild type and mutant HREs (Table 1) were cloned into the TATA-box containing pLuc-MCS vector (Stratagene) as double-stranded oligonucleotides and verified by sequencing. The 4x*EPO* HRE construct contains 4 copies of the *EPO* long sequence (Table 1), separated by a linker sequence, in pLuc-MCS. The CMV-luc construct has the immediate-early CMV promoter in pGL2 basic (Promega). The HIF-1α(P402A, P564A) and HIF-2α(P405A, P531A) mutants were generated by PCR and cloned into the pcDNA3 expression vector (Invitrogen).

Cell culture and transient transfection assay

Saos-2 cell line was maintained as described previously [8]. The Chinese hamster ovary (CHO) cell lines C 4.5 (control) and Kal 3.5 (HIF-α deficient), kindly provided by Dr. P. J. Ratcliffe, were grown as described in [9]. Cells, seeded in triplicates, were co-transfected with an HRE-driven firefly luciferase reporter construct and pRL-CMV (Promega), expressing *Renilla* luciferase (internal control for transfection efficiency), using the Effectene reagent (QIAGENE) as described [8]. Activity of each construct was expressed as the average ratio of firefly to *Renilla* luciferase activities (+S.D.).

Biotinylated probe pull down

For high stringency pull down [6] nuclear extract was prepared from normoxic and hypoxic (0.5% O_2) Saos-2 cells with NE-PER kit (Pierce). Streptavidin–Sepharose (Stratagene) was washed three times in phosphate- buffered saline (pH 7.4)/0.1% BSA and two times with Tris–EDTA (TE, pH 8.0)/1M NaCl and used (40 μl of 50% slurry) to immobilize 40 pmol double-stranded probes (top strand biotinylated at the 5′-end Table 1) in TE/1M NaCl (500 μl). After rotating for 20 min (all incubations were at room temperature), Sepharose was washed three times with the same buffer and two times with 1× binding buffer (10 mM Tris (pH 7.6), 50 mM KCl, 1 mM $MgCl_2$, 1 mM EDTA, 5 mM DTT, 5% glycerol, .03% Nonidet P-40). Nuclear proteins (60 μg), preincubated for 5 min with 2.5 μg of poly (dI–dC) in 100 μl 1× binding buffer/1 mM sodium orthovanadate, were rotated with 10 μl Sepharose/probe for 20 min. Sepharose was then washed three times with 1× binding buffer/0.5 μg/ml poly(dI–dC), resuspended in 1× sample buffer, boiled, and bound proteins were separated by SDS–PAGE.

Western blotting and staining of biotinylated probes

Expression of the HIF-1α(P402A, P564A) and HIF-2α(P405A, P531A) mutants in transiently transfected cells was probed by Western blotting as described previously [8], using HIF-1α monoclonal (BD Biosciences) and HIF-2α polyclonal (Novus) antibody, respectively. β-Actin (Sigma) was used as internal control. HIF-1α in pull down experiments was also detected by Western blotting. Equal amount of biotinylated double-stranded probes was confirmed by electrophoresis in 12% non-denaturing gel, blotting onto Hybond N+ membrane (Amersham Biosciences), and detection with Streptavidin-Peroxidase Polymer (Sigma) and Enhanced Chemiluminescence (ECL) kit (Pierce).

Results and discussion

Hypoxic induction of selected endogenous HREs

Initially, we studied hypoxic induction of a single copy of endogenous HREs upstream of a minimal TATA-box in transiently transfected Saos-2 cells. We used 29 bp-long sequences (23 bp in the case of m*PGK1* HRE), excluding thus contribution of transcription factors that cooperate with HIF in the longer forms of some HREs [7,10,11]. Among the tested HREs, m*LDHA* and m*PGK1* HREs yielded by far the strongest hypoxic induction (199 and 80×, respectively, Fig. 1A). Interestingly, the HBS containing fragment from the gene coding for carbonic anhydrase IX (CA IX), one of the intrinsic markers of cellular hypoxia [12], displayed a remarkably low induction (1.7×), one of the lowest among the HREs tested (Fig. 1A). The CCCGCAC sequence in m*LDHA* HRE (Table 1) closely resembles the SP1/SP3-binding GC-box [13]. Although its functionality has not been formally confirmed, the synergistic cooperation between the SP1 site and HBS in *CA9* HRE [11] prompted us to test its role in m*LDHA* HRE function. Mutations eliminating SP1/SP3-binding (Table 1) [13] failed to affect m*LDHA* HRE activity (data not shown), meaning that not only the GCbox-like motif does not contribute to hypoxic induction but also that mutations between the two HBSs do not significantly affect HRE activity. Reversing the orientation did not affect activity of either m*LDHA* or m*PGK1* HREs (data not shown). In conclusion, hypoxic induction of m*LDHA* and m*PGK1* HREs indicated that their *cis*-acting element(s) are sufficient for effective recognition by the HIF system and therefore these two HREs were selected for further study.

Structural organization of mLDHA and mPGK1 HREs

m*LDHA* and m*PGK1* HREs have in common two HBSs (GTCGTG in m*PGK1* HRE will be considered as an imperfect HBS). In m*PGK1* HRE, the arrangement of HBSs is parallel (par) (Fig. 1B). Formally, because of the symmetry of CACGTG, HBSs in m*LDHA* HRE could be par, with increased spacing between HBSs compared to m*PGK1* HRE (solid and dashed arrows in Fig. 1B), or antiparallel (a-par) (solid arrows in Fig. 1B). In order to find the functional arrangement, we mutagenized the −2 positions (Fig. 1C) of CACGTG. As magnitude of hypoxic induction decreases in the T ≫ G > C order [2], we reasoned that introduction of T into the weak CACGTG would enhance activity only in the −2 position of the functional arrangement. Relative to the proximal HBS, TACGTG in mut1 (asterisk in Fig. 1B) is par, but it becomes CACGTA (disrupting the core HBS sequence) in the a-par arrangement, whereas in mut2 (triangle in Fig. 1B) the situation is reversed. Considerably lower activity of mut1, compared to the wild type or mut2 (Fig. 2A), confirmed that the functional arrangement of HBSs in m*LDHA* HRE is a-par. We conclude that HIF can effectively transactivate two fundamentally different arrangements of HBSs: par and a-par.

Optimization of mLDHA and mPGK1 HREs

Next, we optimized m*LDHA* and m*PGK1* HREs. As all HBSs in these two HREs have a suboptimal G or C nucleotide at the −2 position (Fig. 1B), we introduced T into these positions plus A at the −1 position of the proximal HBS in m*PGK1* HRE (Table 1). Mutations indeed stimulated hypoxic activity and HREs with the double T replacement (mut3) were the most active (Fig. 2A and B). Thus, optimization of HBSs stimulates hypoxic induction of both a-par (m*LDHA* HRE) and par (m*PGK1* HRE) arrangements.

Deletion/insertion mutants were used to evaluate the effect of spacing between HBSs. In m*LDHA* HRE mut3 (a-par), deletion of a single nucleotide (mut4) was tolerated, whereas insertion of a single nucleotide (mut5) decreased activity considerably (Table 1, Fig. 2C). Deletion (mut6) and insertion (mut7) of 3 nucleotides abrogated the synergy between HBSs (Table 1, Fig. 2C). In contrast, m*PGK1* HRE mut3 (par) appears to be significantly more sensitive to altered spacing between HBSs as deletion (mut4) and insertion (mut5) of a single

nucleotide drastically reduced hypoxic induction (Table 1, Fig. 2D). Apparently, HBSs in m*PGK1* HRE (and presumably other par arrangements) are “locked”, as the slightest alteration of spacing had a profound inhibitory effect on hypoxic activity. The a-par arrangement appears to be more flexible as it tolerated some alterations. Based on these data, the optimal spacing between HBSs is 10 bp for the par and 16 bp (from positions 1) for the a-par arrangement (Fig. 1B). Structurally, par HBSs positioned 10 bp apart are on the same side of DNA and the larger distance in the a-par arrangement is presumably required for similar favorable alignment when HBSs reside on separate strands. Previously, we noted a remarkably low hypoxic activity of a construct with three copies of the *EPO* HBS (par) 20 bp apart (Kaluz, unpublished). In our opinion, the low activity of this construct, m*LDHA* HRE mut1 (this study), and multimerized m*LDHA* HBSs in the earlier report [7] reflects the suboptimal (longer) spacing between the HBSs. Therefore, spacing between HBSs is a critical determinant of HRE activity and, for the purpose of constructing minimal enhancers, spacing between HBSs in m*LDHA* and m*PGK1* HREs is optimal (providing maximal activity).

Finally, we studied the effect of spacing between the TATA-box and the HRE. Constructs described so far had 35 (m*LDHA*) and 34 (m*PGK1*) bp spacing between the proximal HBS and the TATA-box (Table 1). Interestingly, increased (47 bp) as well as decreased (33 and 15 bp) (Table 1) spacing invariably downregulated hypoxic induction of m*LDHA* HRE mut3 (Fig. 2E). The lowest activity of the mutant with 15 bp spacing (about two helical turns shorter than in the optimal construct) was relatively unexpected and suggested that cooperation between HREs and the TATA-box is more complex and may involve additional features, e.g., DNA bending. Increased spacing (46 bp) had a similar negative effect on m*PGK1* HRE mut3 (data not shown). Therefore, the distance between the HRE and the TATA-box also affects hypoxic activation and there is an optimal spacing between the two.

Design and characterization of minimal hypoxia-inducible enhancers

Optimizations enhanced hypoxic induction of both types of HREs, but the overall activity generated by two optimized HBSs was still rather low. Having established the optimal spacing between HBSs, we considered ways to assemble artificial minimal enhancers exclusively from optimized HBSs. Three copies can be arranged a-par, par (the a-par arrangement gave consistently higher activity) or par, par (Table 1). Surprisingly, the construct with the former arrangement, assembled from m*LDHA* HRE mut3 and a TACGTGcag HBS (Table 1), produced even lower activity than the parental m*LDHA* HRE mut3 construct (Fig. 3A). In contrast, the par, par construct, assembled from 3 copies of the TACGTGcag HBS (Table 1), provided robust hypoxic induction, considerably higher than constructs with two HBSs (Fig. 3A), confirming that even odd numbers of properly arranged HBSs can generate a strong synergistic effect. This proves that the most efficient way of arranging HBSs is par.

Next, we compared constructs with increasing numbers of par arranged optimized HBSs. Strong synergistic effects were observed with addition of each HBS, resulting in high hypoxic activity of constructs with 3 and 4 HBSs (Fig. 3B). The 4xopt HBS construct (total 36 bp) performed comparably to the 4x*EPO* HRE construct (total 208 bp) (Fig. 3B), confirming that HIF activates properly multimerized optimized HBSs in a way similar to multimers of the much longer endogenous *EPO* HRE. Activity of the 4xopt HBS construct in hypoxia was almost as high as activity of the CMV promoter (~800 bp, Fig 3B). HIF-1α and HIF-2α differ in transactivation of some hypoxia-inducible genes, e.g., expression of glycolytic enzymes (such as PGK1) is preferentially activated by HIF-1α [14]. Par arrangement of HBSs in our enhancers, originally present in m*PGK1* HRE, prompted us to test the transactivation potential of HIF-1α and HIF-2α on the 4xopt HBS and 4x*EPO* HRE constructs. HIF-1α(P402A, P564A) and HIF- 2α(P405A, P531A) mutants comparably activated both constructs (Fig. 3C),

suggesting that HIF-1α and HIF-2α are equally efficient in transactivation of multimers of optimized HBSs and endogenous *EPO* HREs.

Comparison of the 4xopt HBS and 4x*EPO* HRE constructs in the HIF-α deficient Kal 3.5 and control C 4.5 CHO cell lines [9] confirmed activation by hypoxia only in C 4.5 cells and considerably lower normoxic activity in Kal 3.5 cells (Fig. 4A). While induction of both constructs by hypoxia was comparable in C 4.5 cells, the 4x*EPO* HRE construct generated higher activity in Kal 3.5 cells and higher normoxic activity in C 4.5 cells (Fig. 4A). Together, these data confirm that hypoxic induction of both constructs strictly depends on HIF and that HIF activity is responsible for increased normoxic activity.

To understand why spacing between the optimized HBSs has such a profound effect on hypoxic induction, we performed pull down experiments with biotinylated double-stranded probes with three HBSs, spaced either optimally (par, par opt) or non-optimally, due to insertions of three nucleotides (par, par, non-opt) (Table 1). Using high stringency washing [6], we found that optimally spaced HBSs pull down significantly more HIF-1α than the non-optimally spaced HBSs from nuclear extract prepared from hypoxic cells (Fig. 4B). Detection with streptavidin-peroxidase confirmed comparable amounts of biotinylated probes used (Fig. 4C). Thus, properly aligned HBSs facilitate cooperative interaction between HIF complexes, resulting in high affinity HIF binding and strong synergistic cooperation.

We had invested a considerable effort into developing hypoxiainducible vectors based on the exceptionally tightly regulated *CA9* promoter [11]. We reasoned that the combination of the TATA-less *CA9* promoter (tight control in normoxia) and minimal hypoxiainducible enhancers (high hypoxic induction) could generate a construct with superior activity. The *CA9* HBS, located immediately upstream of the transcription start site [11], allows assembling a chimeric promoter that consists entirely of a single type of regulatory element—HBS. However, regardless of the arrangement of HBSs, activity of all of the *CA9* chimeric promoter constructs was always considerably lower than that of the TATA-box containing m*LDHA* HRE mut3 construct (data not shown). This presumably reflects that HBSs on their own are deficient in activation of transcription and reiterates the importance of the synergistic cooperation between HBSs and the TATA-box.

In addition to using optimized HBSs, the fundamental difference between the minimal hypoxia-inducible enhancers described in this study and the multimers of endogenous HREs lies in the building blocks used. By definition, the building block in multimerized HRE is the whole endogenous HRE of varying length, linked together via spacer sequences [4]. Resulting increased spacing (longer than the optimal 10 bp for the par arrangement) prevents/decreases synergism between HBSs in the neighboring HREs. In minimal hypoxia-inducible enhancers, the building block is the optimized HBS that is multimerized at the same, optimal distance, ensuring maximal synergism between any two neighboring HBSs. This effectively generates a series of overlapping HREs and maximizes activity for any given number of HBSs. Although in this study, we sought maximal activity, we can also envisage fine-tuning of activity of these enhancers by mutating (“de-optimizing”) individual positions in HBSs.

In conclusion, by using the Occam’s razor, we have designed artificial minimal hypoxia-inducible constructs, consisting of a minimal TATA-box and optimally arranged optimized HBSs. These constructs are highly inducible by hypoxia, proving, contrary to the previous reports, that properly arranged HBSs are sufficient for hypoxic activation. Our work improves understanding of the basic structural determinants of HREs and pioneers the combinatorial approach that will have implications for designing new generation of hypoxiainducible vectors.

Abbreviations

A-par
antiparallel

CA9
carbonic anhydrase 9

CHO
Chinese hamster ovary

CP
ceruloplasmin

EPO
erythropoietin

ECL
enhanced chemiluminescence

ET
endothelin

HBS
HIF-binding site

HIF
hypoxia-inducible factor

HRE
hypoxia-responsive element

m*LDHA*
murine *lactate dehydrogenase-A*

m*PGK1*
murine *phosphoglycerate kinase-1*

PAI
plasminogen activator inhibitor-1

Par
parallel

r*Glut1*
rat *glucose transporter-1*

STRA13
stimulated with retinoic acid-13

VEGF
vascular endothelial growth factor

References

1. Wenger RH, Stiehl DP, Camenish G. Integration of oxygen signaling at the consensus HRE. Sci STKE 2005;306:re12. [PubMed: 16234508]

2. Ameri K, Burke B, Lewis CE, Harris AL. Regulation of a rat VL30 element in human breast cancer cells in hypoxia and anoxia: role of HIF-1. Br J Cancer 2002;87:1173–1181. [PubMed: 12402159]
3. Kimura H, Weisz A, Ogura T, Hitomi Y, Kurashima Y, Hashimoto K, D'Acquisto F, Makuuchi M, Esumi H. Identification of hypoxia-inducible factor 1 ancillary sequence and its function in vascular endothelial growth factor gene induction by hypoxia and nitric oxide. J Biol Chem 2001;276:2292–2298. [PubMed: 11056166]
4. Boast K, Binley K, Iqball S, Price T, Spearman H, Kingsman S, Kingsman A, Naylor S. Characterization of physiologically regulated vectors for the treatment of ischemic disease. Hum Gene Ther 1999;10:2197–2208. [PubMed: 10498251]
5. Post DE, Van Meir EG. Generation of bi-directional hypoxia/HIF-responsive expression vectors to target gene expression to hypoxic cells. Gene Ther 2001;8:1801–1807. [PubMed: 11803400]
6. Ebert BL, Bunn HF. Regulation of transcription by hypoxia requires a multiprotein complex that includes hypoxia-inducible factor 1, an adjacent transcription factor, and p300/CREB binding protein. Mol Cell Biol 1998;18:4089–4096. [PubMed: 9632793]
7. Firth JD, Ebert BL, Ratcliffe PJ. Hypoxic regulation of lactate dehydrogenase A: interaction between hypoxia inducible factor 1 and cAMP response elements. J Biol Chem 1995;270:21021–21027. [PubMed: 7673128]
8. Kaluzová M, Kaluz S, Lerman MI, Stanbridge EJ. DNA damage is a prerequisite for p53-mediated proteasomal degradation of HIF-1alpha in hypoxic cells and downregulation of the hypoxia marker carbonic anhydrase IX. Mol Cell Biol 2004;24:5757–5766. [PubMed: 15199132]
9. Wood SM, Wiesener MS, Yeates KM, Okada N, Pugh CW, Maxwell PH, Ratcliffe PJ. Selection and analysis of a mutant cell line defective in the hypoxiainducible factor-1α-subunit (HIF-1 α). J Biol Chem 1998;273:8360–8368. [PubMed: 9525945]
10. Galson DL, Tsuchiya T, Tendler DS, Huang LE, Ren Y, Ogura T, Bunn HF. The orphan receptor hepatic nuclear factor 4 functions as a transcriptional activator for tissue-specific and hypoxia-specific erythropoietin gene expression and is antagonized by EAR3/COUP-TF1. Mol Cell Biol 1995;15:2135–2144. [PubMed: 7891708]
11. Kaluz S, Kaluzová M, Stanbridge EJ. Expression of the hypoxia marker carbonic anhydrase IX is critically dependent on SP1 activity. Identification of a novel type of hypoxia-responsive enhancer. Cancer Res 2003;63:917–922. [PubMed: 12615703]
12. Potter C, Harris AL. Hypoxia inducible carbonic anhydrase IX, marker of tumour hypoxia, survival pathway and therapy target. Cell Cycle 2004;3:64–167. [PubMed: 14657668]
13. Shi Q, Le X, Abbruzzese JL, Peng Z, Qian C-N, Tang H, Xiong Q, Wang B, Li X-C, Xie K. Constitutive Sp1 activity is essential for differential constitutive expression of vascular endothelial growth factor in human pancreatic adenocarcinoma. Cancer Res 2001;61:4143–4154. [PubMed: 11358838]
14. Hu CJ, Wang LJ, Choodosh LA, Keith B, Simon MC. Differential roles of hypoxia-inducible factor 1α (HIF-1α) and HIF-2α in hypoxic gene regulation. Mol Cell Biol 2003;23:9361–9374. [PubMed: 14645546]

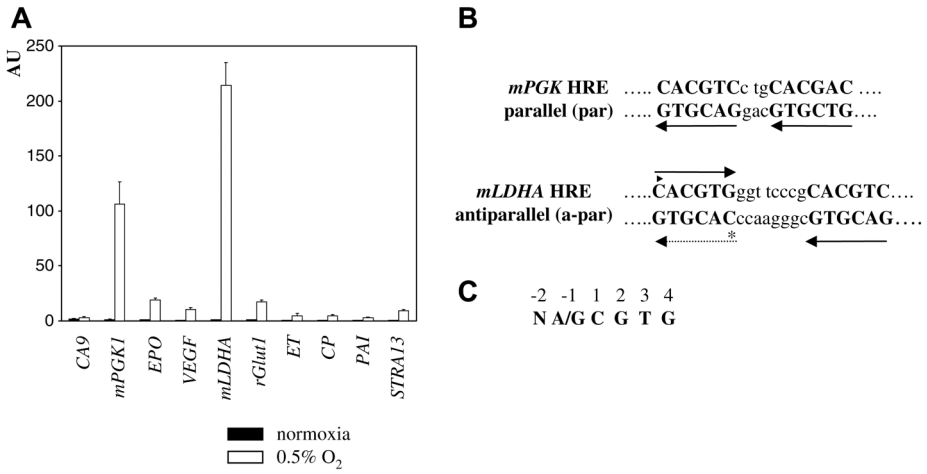

Fig. 1.

(A) Hypoxic induction of selected wild type HREs. HREs in pLucMCS were co-transfected with pRL-CMV into Saos-2 cells for 16 h, followed by exposure to 0.5% O_2 for 24 h. Promoter activities are expressed as the ratio of firefly/*Renilla* activity in arbitrary units (AU), each of the bars representing the mean value ($X \pm$ SD) from three experiments. *CA9*, *carbonic anhydrase 9*; m*PGK1*, murine *phosphoglycerate kinase-1; EPO*, *erythropoietin; VEGF*, *vascular endothelial growth factor*; m*LDHA*, murine *lactate dehydrogenase-A*; r*Glut1*, rat *glucose transporter-1; ET*, *endothelin; CP*, *ceruloplasmin; PAI*, *plasminogen activator inhibitor-1; STRA13*, *stimulated with retinoic acid-13* (B) Schematic outline of HBS arrangements in m*LDHA* and m*PGK1* HREs and their designation. Arrows indicate the orientation of HBSs. (C) Numbering of positions in HBS.

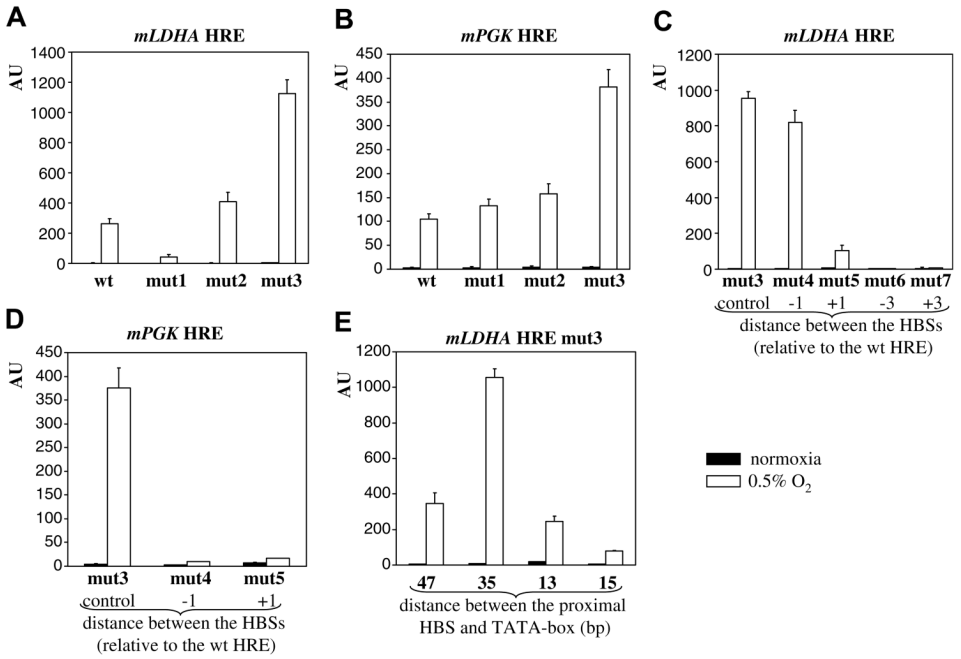

Fig. 2.

Optimization of m*LDHA* and m*PGK1* HREs. Optimization of the −2 positions of m*LDHA* (A) and m*PGK1* HREs (B). The effect of HBS spacing on activity of m*LDHA* (C) and m*PGK1* (D) HRE. The effect of spacing between HRE and TATA-box on activity of m*LDHA* mut3 (E). Transfection and expression of promoter activities were as described in Fig. 1.

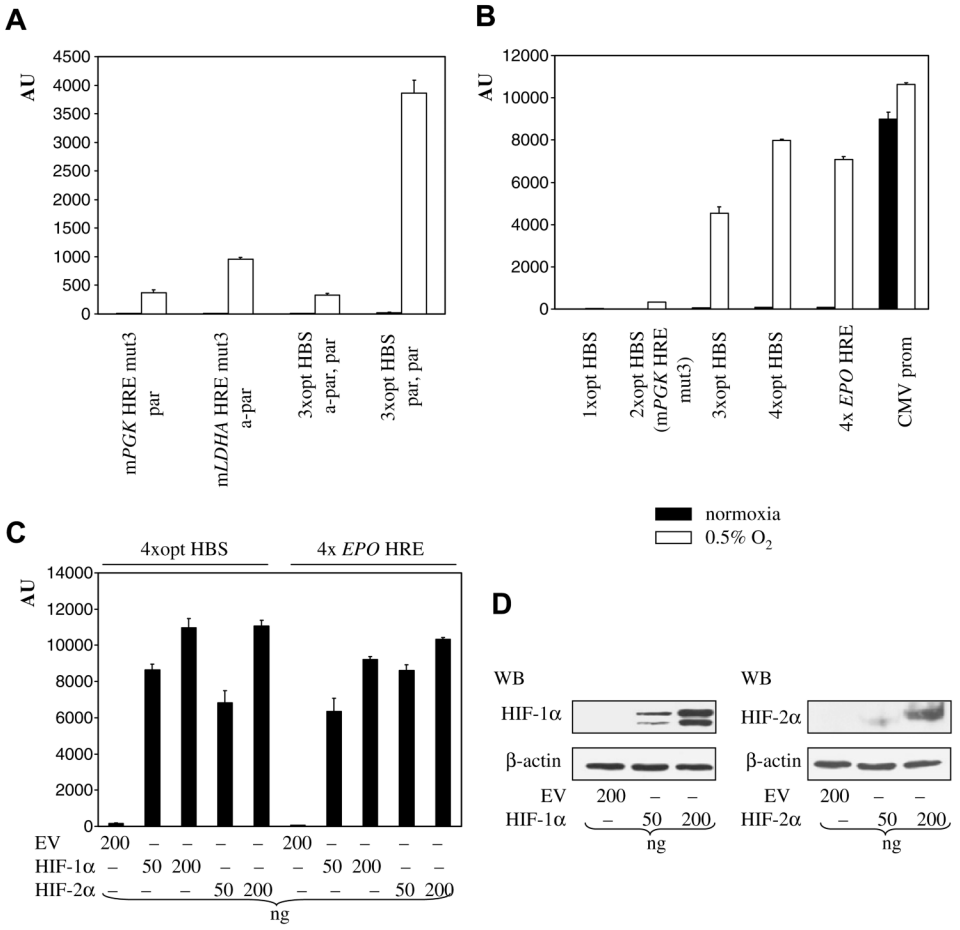

Fig. 3.

Design and activity of minimal hypoxia-inducible enhancers. The effect of arrangement of three HBSs (A), increasing number of HBSs in par arrangement (B), cotransfection of HIF-1α(P402A, P564A) and HIF-2α(P405A, P531A) mutants (C) on reporter activity. Transfection and expression of promoter activities were as described in Fig. 1. Production of HIF-1α(P402A, P564A) and HIF-2α(P405A, P531A) mutants was evaluated by Western blotting (D).

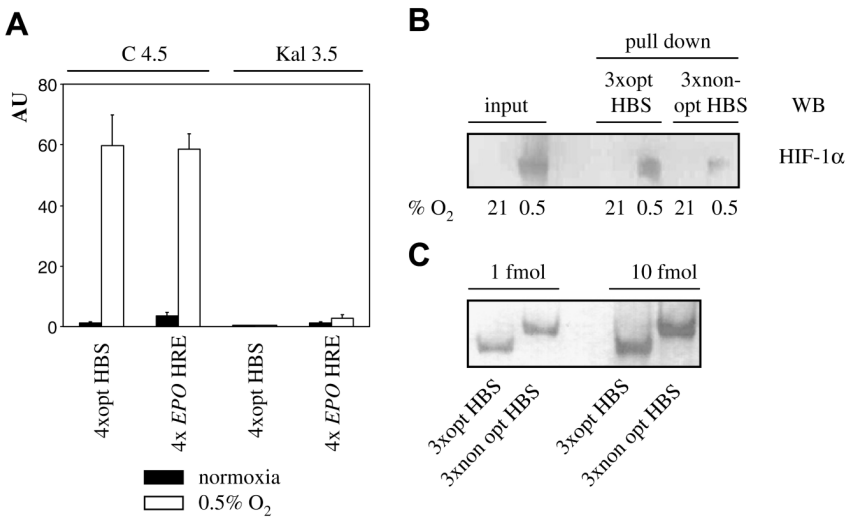

Fig. 4.

(A) Activity of 4xopt HBS and 4x*EPO* HRE constructs in HIF-α deficient Kal 3.5 and control C 4.5 CHO cells. Transfection and expression of promoter activities were as described in Fig. 1. (B) Pull-down with biotinylated double-stranded probes comprising three copies of HBSs with optimal and non-optimal (+3) spacing. Bound nuclear proteins were washed under high stringency and analyzed for HIF-1α by Western blotting. (C) Indicated amounts of biotinylated double-stranded probes were subjected to electrophoresis, blotted, and detected with streptavidin-peroxidase and ECL.

Table 1

Sequences used in this study, written in the 5′;–3′ direction

wt HREs:

STRA13	GGCCAGACGTGCCTGGAGTCACAGGGTAG
rGlut1	CCACAGGCGTGCTGGCTGACACGCATCAG
mPGK1	TTTGTCACGTCCTGCACGACGCG
PAI	GTGTGTACGTGGTAAGAGCATTCAGGAAC
CP	ATCTGTACGTGACCACACTCACCTCTAAA
ET	CAGGCAACGTGCAGCCGGAGATAAGGCCA
CA9	GGCTGTACGTGCATTGGAAACGAGAGCTG
mLDHA	GCCTACACGTGGGTTCCCGCACGTCCGCT
EPO	GGCCCTACGTGCTGTCTCACACAGCCTGT
EPO long	GGCCCTACGTGCTGTCTCACACAGCCTGTCTGACCTCTCGACCT
VEGF	GTGCATACGTGGGCTCCAACAGGTCCTCT

Mutant m*LDHA* HREs:

wt	GCCTACACGTGGGTTCCCGCACGTCCGCT
SP1mut	GCCTACACGTGGGTTC**AA**GCACGTCCGCT
mut1	GCCTACACGT**A**GGTTCCCGCACGTCCGCT
mut2	GCCTA**T**ACGTGGGTTCCCGCACGTCCGCT
mut3	GCCTA**T**ACGTGGGTTCCCGCACGT**A**CGCT
mut4	GCCTA**T**ACGTGGGTT CCGCACGT**A**CGCT
mut5	GCCTA**T**ACGTGGGTT**a**CCCGCACGT**A**CGCT
mut6	GCCTA**T**ACGTGGG CCGCACGT**A**CGCT
mut7	GCCTA**T**ACGTGGGTT**ctt**CCCGCACGT**A**CGCT

Mutant m*PGK1* HREs:

wt	TTTGTCACGTCCTGCACGACGCG
mut1	TTTGTCACGTCCTGCACG**TA**GCG
mut2	TTTGTCACGT**A**CTGCACGACGCG
mut3	TTTGTCACGT**A**CTGCACG**TA**GCG
mut4	TTTGTCACGT**A** TGCACG**TA**GCG
mut5	TTTGTCACGT**At**CTGCACG**TA**GCG

Sequence between the proximal HBS of m*LDHA* HRE mut3 and the TATA-box (counted from the position 1 of the proximal HBS and the first T of the TATA-box, both underlined bold)**:**

mut3 (47)	**G**TACGCTCGCTGATCTCTCGAGGTCGACAGCGGAGACTCTAGAGGG***T****ATATA*
mut3 (35)	**G**TACGCTCGCT TCGACAGCGGAGACTCTAGAGGG***T****ATATA*
mut3 (33)	**G**TACGCTCGCT GATCTCTCGAGATCTAGAGGG***T****ATATA*
mut3 (15)	**G**TACGCTCGCT GGG***T****ATATA*

Sequences of multimers of 3 copies of optimized HBSs:

a-par, par	**TACGTG**GGTTCCCG**CACGTA**CTG**CACGTA**
par, par opt	biotin-CTG**CACGTA**CTG**CACGTA**CTG**CACGTA**
par, par non-opt	biotin-CTG**CACGTA**aagCTG**CACGTA**aagCTG**CACGTA**

Mutations against wt sequences are indicated in underlined bold, small cap letters indicate insertions, TATA-box and other *cis*-acting elements are in italics.

Mutations against wt sequences are indicated in underlined bold, small cap letters indicate insertions, TATA-box and other *cis*-acting elements are in italics.